

Effect of pressure on the mechanisms of the CO₂/H₂ reaction on a CO-precipitated CuO/ZnO/Al₂O₃ catalyst

Rachid Sahki · Ouarda Benlounes · Ouiza Chérifi · René Thouvenot · Mohammed M. Bettahar · Smain Hocine

Received: 18 December 2010/Accepted: 23 March 2011/Published online: 27 April 2011
© The Author(s) 2011. This article is published with open access at Springerlink.com

Abstract The influence of working pressure on the mechanisms of the CO₂/H₂ reaction on a co-precipitated CuO/ZnO/Al₂O₃ catalyst have been studied at 230 °C and in the pressure range of 1–75 bar. In the CO₂ hydrogenation using CuO/ZnO/Al₂O₃, the products were found to be CO, methanol and water almost exclusively. Only a trace of methane formation was observed. Methanol and carbon monoxide are competitively formed. The former is produced directly from CO₂ whatever the pressure whereas carbon monoxide stems either from CO₂ directly at high pressure or both methanol decomposition and CO₂ directly at low pressure.

R. Sahki · O. Benlounes · S. Hocine (✉)

Laboratoire de Chimie Appliquée et de Génie Chimique Université M. Mammeri de Tizi-Ouzou,
BP17 R.P. 1500, Tizi-Ouzou, Algeria
e-mail: shocine_univ_to@yahoo.fr

R. Sahki

e-mail: rasahki@yahoo.fr

O. Benlounes

e-mail: ouardabenc@yahoo.fr

O. Chérifi

Laboratoire de Chimie du Gaz Naturel, Institut de Chimie BP32, El-Alia, 16111 Bab-Ezzouar,
Alger, Algeria
e-mail: ouizac@yahoo.fr

R. Thouvenot

Institut Parisien de Chimie Moléculaire, UMR 7201, Equipe Polyoxometallates, Case Courier 42,
Université Pierre et Marie Curie, 4 Place Jussieu, 75252 Paris cedex 05, France
e-mail: rene.thouvenot@upmc.fr

M. M. Bettahar

UMR CNRS 7565 Catalyse Hétérogène/Structure Organique et Réactivité Faculté des Sciences
Université Henri Poincaré, Nancy I Boulevard des Aiguillettes BP 70239, 54506 Vandoeuvre-lès-
Nancy, France
e-mail: Mohammed.Bettahar@lcah.uhp-nancy.fr

Keywords Methanol · Mechanism · CO₂/H₂ · Cu–ZnO–Al₂O₄

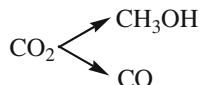
Introduction

Carbon dioxide is accumulating more and more in the atmosphere and seems to participate to the so-called green-house effect. So the reduction of this waste is of great interest. The simplest way to utilize carbon dioxide is its hydrogenation into valuable compounds such as methanol, generally on copper based catalysts. The synthesis of methanol from CO/CO₂/H₂ mixtures using CuO/ZnO/Al₂O₃ catalysts is currently attracting much interest due to its economical importance [1–7]. As this reaction produces methanol and carbon monoxide competitively, the role of each oxide in the mechanism of methanol formation (reactions 1 and 2) is still a matter of debate [8–11] since the reaction of conversion (reaction 3) also occurs: (1), hydrogenation of carbon dioxide, (2) the hydrogenation of carbon monoxide (3) water–gas shift reaction.



According to Klier [8, 9] (CuO/ZnO = 30/70, 250 °C, 75 bar), carbon monoxide is the principal source of methanol production (reaction 1). However, Schack et al. [10] suggested that carbon monoxide hydrogenation is the main route to methanol at typical industrial conditions while carbon dioxide is the main route under lower temperatures and pressures. According to Chinchen et al. [11] (industrial CuO/ZnO/Al₂O₃ = 60/30/10 catalyst, 250 °C, 50 bar), methanol is directly formed from carbon dioxide. Using isotopic labeling to determine the main reaction that occurs in the methanol synthesis under the typical industrial conditions of 250 °C and 5.2 MPa, Chinchen et al. [12] found that the methanol produced had the same ¹⁴C as that of carbon dioxide used in the feed gas. Therefore, this points out that methanol is directly produced from carbon dioxide immediately whereas carbon monoxide is first converted to carbon dioxide via the reverse water gas shift reaction and carbon dioxide remains the principal source of methanol. A study by Lee et al. [13] asserted that carbon dioxide hydrogenation to methanol is the dominant reaction. On the other hand, the results reported by Liu et al. [14] (CuO/ZnO = 30/70, 220 °C, 17 bar) indicate that methanol originates from the hydrogenation of both of the two carbon oxides.

Due to these conflicting results, the synthesis of methanol from the hydrogenation of CO₂ on the same catalysts has also received attention [15–19]. Indeed, this reaction competitively produces methanol and carbon monoxide and thus, due to the occurrence of the above reactions (1–3), the problem of carbon source of methanol is also posed. Rosovskii et al. [20] (CuO/ZnO/Al₂O₃ SNM1 industrial catalyst, 250 °C, 50 bar) as well as Bardet et al. [21] (CuO/ZnO/Al₂O₃ academic catalyst, 250 °C, 1 bar) concluded that the products are formed by parallel reactions (Reaction 1):



Reaction 1

In the earliest work of Ipatieff ($\text{CuO}/\text{Al}_2\text{O}_3$ catalyst, $300\text{ }^\circ\text{C}/400\text{ bar}$) [18], it is proposed that methanol is produced by the intermediary of carbon monoxide through a successive reaction path (Reaction 2):

However, the results obtained on the CuO/MgO and CuO/ZrO_2 catalysts at $20\text{ }^\circ\text{C}/1\text{ bar}$ [19] as well as those achieved on $\text{CuO}/\text{ZnO}/\text{Al}_2\text{O}_3$ catalysts at $230\text{ }^\circ\text{C}/1\text{ bar}$ [22] contradictorily show that a second type of successive reactions occurs in the CO_2/H_2 in which methanol is the primary product (Reaction 3):

The above reported results about the synthesis of methanol in both the $\text{CO}/\text{CO}_2/\text{H}_2$ and the CO_2/H_2 reactions let us think that the different proposed mechanisms may be related to different solids and, even, to different operating conditions. The present work deals with the influence of pressure on the kinetics of the CO_2/H_2 reaction on a co-precipitated $\text{CuO}/\text{ZnO}/\text{Al}_2\text{O}_3$ catalyst. The method of investigation is the variation of the relative selectivity $\gamma = [\text{CH}_3\text{OH}]/[\text{CO}]$ as a function of the contact time [19, 20].

Experimental

Catalyst preparation

The catalyst was prepared by co-precipitating a solution of copper and zinc nitrates with sodium carbonate at $80\text{ }^\circ\text{C}$. At $\text{pH} = 7$, 10% Al_2O_3 was added to the co-precipitate. The resulting $\text{Cu}/\text{Zn}/\text{Al}$ suspension was centrifuged and the obtained precipitate was dried at $110\text{ }^\circ\text{C}$ and calcined for 3.5 h under air at $350\text{ }^\circ\text{C}$ after a $100\text{ }^\circ\text{C}\text{ h}^{-1}$ heating rate treatment. The copper, zinc and aluminum contents of the calcined solid were 21.7, 50.0 and 4.1% respectively. The detected impurities were as follows (ppm): Mg(<80), Ca(<80), Na(<90), Fe(<90).

Catalyst characterization

The surface area of the oxidized precursor was $29.4\text{ m}^2\text{ g}^{-1}$. Its XRD spectra show well defined bands of expected phases: CuO , ZnO and $\delta\text{-Al}_2\text{O}_3$, whereas the presence of no decomposed carbonates phases is observed by IR spectroscopy. The copper surface area was $2.0\text{ m}^2\text{ g}^{-1}$ and has been determined by N_2O decomposition using a pulse technique as described by Evans [23].



Reaction 2



Reaction 3

Kinetic study

The catalyst testing was carried out in a stainless steel reactor (Sotelem RDP). The sample (0.2 g) was reduced in flowing H₂ (1.3 L min⁻¹) by heating at 20 °C min⁻¹ to 300 °C and holding at this temperature for 16 h. The temperature was then lowered to the reaction temperature (230 °C) and the reactor was fed with the reaction mixture: CO₂/H₂ = 1/3. The total flow rate was in the range 0.3–3.6 L h⁻¹ and the operating pressures were 1, 20, 28, 35, 50, and 75 bar. Reactants and products were analyzed on line using TCD and FID chromatographs equipped with Carbosieve and porapak Q columns. The results are expressed as a function of the reciprocal of the flow-rate 1/d (h L⁻¹).

Results and discussion

The hydrogenation of carbon dioxide over supported cooper catalysts produces both carbon monoxide and methanol, and the influence of pressure on the activity and selectivity of the reaction was examined. The catalyst activity was tested at 1, 20, 28, 35, 50, 75 bar, 230 °C, and a flow-rate of 2 L h⁻¹. Data for the conversion of CO₂ and selectivities of methanol and CO during 16 h on-stream with the CuO/ZnO/Al₂O₃ catalyst are given in Fig. 1. When the CO₂/H₂ mixture was fed over the catalyst, methanol was produced together with carbon monoxide and water. The catalyst was stable after about 3 h on stream and so the results refer to a steady state situation. With an increase in the pressure, the CO₂ conversion and methanol selectivity increased, and the CO selectivity decreased considerably. At 230 °C and a flow-rate of 2 L h⁻¹, the CO₂ conversion increases from 3.1 to 11.9% when the total pressure is raised from 1 bar to 75 bar. In the same range of pressure, the

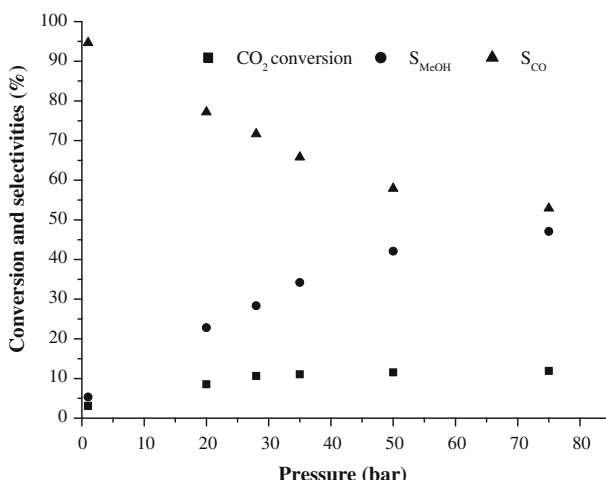


Fig. 1 Variation of CO₂ conversion, S_{CH₃OH} and S_{CO} as a function of pressure at 230 °C for the CuO/ZnO/Al₂O₃ catalyst

methanol selectivity increased from 5.3 to 47.1% and carbon monoxide selectivity decreased from 94.66 to 52.9%.

Through Fig. 1, carbon monoxide is predominant at low pressure, unlike methanol, which is favored at high pressure. This result shows that carbon dioxide is transformed into carbon monoxide at low pressure via the reverse water gas shift reaction (RWGS: reaction 4) occurring simultaneously with methanol formation over the Cu/ZnO/Al₂O₃ catalyst, or could be formed from methanol decomposition, whereas at high pressure CO₂ is converted to methanol. Generally, in the methanol synthesis (reaction 1) from CO₂ hydrogenation, the reverse water gas shift (RWGS: reaction 4) also occurs simultaneously. Therefore, reactions 1 and 4 make the total reaction system of methanol synthesis.



The literature suggests two possible reaction pathways for CH₃OH synthesis from CO₂ and H₂ over the CuO/ZnO/Al₂O₃ catalyst: (i) Formate route, where the reaction proceeds through the formation of formate (HCOO), dioxomethylene (H₂COO), formaldehyde (CH₂O), methoxy (CH₃O) and the final product, CH₃OH [24–26]. This species was commonly detected in experiments [26, 27]. (ii) The pathway involves the reverse water–gas-shift (RWGS, reaction 4) reaction, where CO₂ is first converted to CO which is then hydrogenated to form methanol (reaction 2). In Order to obtain more insight into the real route to methanol in the CO₂/H₂ reaction, we studied the variation of the ratio $\gamma = [\text{CH}_3\text{OH}]/[\text{CO}]$, or its reciprocal $1/\gamma$, as a function of the contact time 1/d. In effect, depending upon involved reaction paths, as the contact time tends to zero, γ should tend towards a finite value for the parallel reactions (Reaction 1), towards zero for the first type of successive reactions (Reaction 2) or towards infinity for the second type of successive reactions (Reaction 3). The obtained results show a great influence of the pressure on the reaction mechanisms. Indeed, as illustrated in Figs. 2, 3, 4 and 5 for the experiments carried out at P = 20, 28, 35 and 75 bar, the behavior of the ratio $\gamma = [\text{CH}_3\text{OH}]/[\text{CO}]$ as a function of the contact time depends strongly on the working pressure.

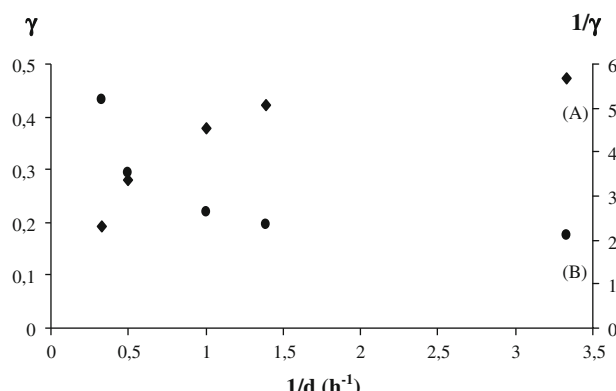


Fig. 2 Variation of the ratio **a** $\gamma = [\text{CH}_3\text{OH}]/[\text{CO}]$ and **b** $1/\gamma = [\text{CO}]/[\text{CH}_3\text{OH}]$ as a function of contact time 1/d at 20 bar and 230 °C for the CuO/ZnO/Al₂O₃

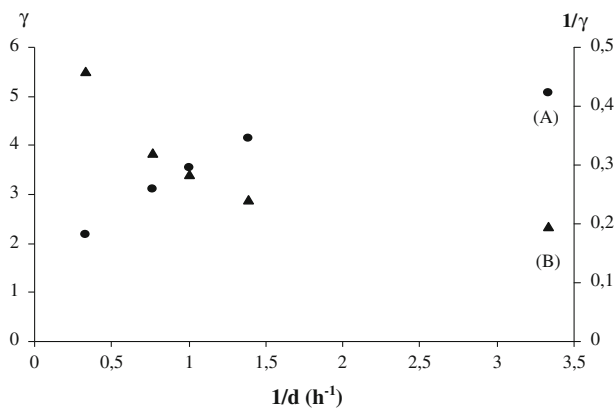


Fig. 3 Variation of the ratio **a** $\gamma = [\text{CH}_3\text{OH}]/[\text{CO}]$ and **b** $1/\gamma = [\text{CO}]/[\text{CH}_3\text{OH}]$ as a function of contact time $1/d$ at 28 bar and 230 °C for the CuO/ZnO/Al₂O₃

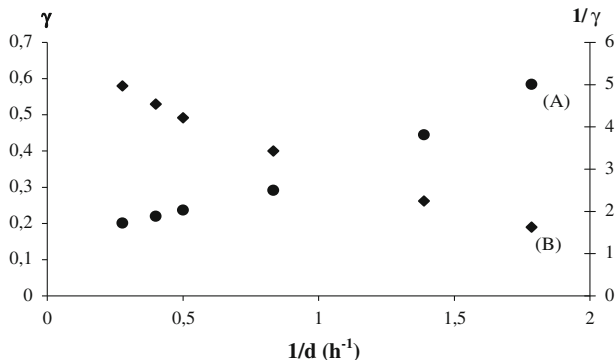


Fig. 4 Variation of the ratio **a** $\gamma = [\text{CH}_3\text{OH}]/[\text{CO}]$ and **b** $1/\gamma = [\text{CO}]/[\text{CH}_3\text{OH}]$ as a function of contact time $1/d$ at 35 bar and 230 °C for the CuO/ZnO/Al₂O₃

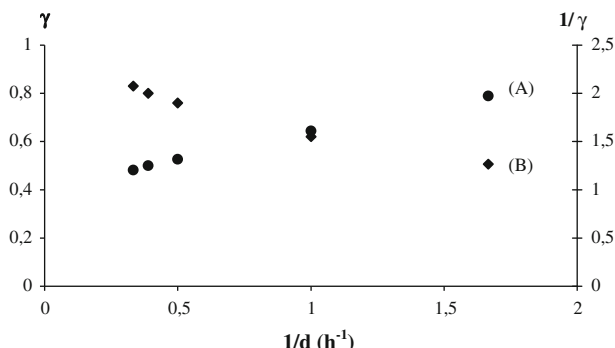


Fig. 5 Variation of the ratio **a** $\gamma = [\text{CH}_3\text{OH}]/[\text{CO}]$ and **b** $1/\gamma = [\text{CO}]/[\text{CH}_3\text{OH}]$ as a function of contact time $1/d$ at 75 bar and 230 °C for the CuO/ZnO/Al₂O₃

Two domains of pressure are to be noted:

- Up to 28 bar, γ increases sharply as $1/d$ tends towards zero (Figs. 2 and 3, curve A) whereas $1/\gamma$ tends towards zero (Figs. 2 and 3, curve B). This implies a reaction mechanism of the type represented in Reaction 3.
- From 35 bar, γ tends towards a finite value as $1/d$ tends towards zero (Figs. 4 and 5, curve A) whereas $1/\gamma$ tends towards a finite value also (Figs. 4 and 5, curve B).

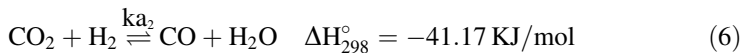
Thus, it appears that carbon dioxide is the immediate precursor of methanol in the CO_2/H_2 reaction whatever the working pressure.

Thermodynamic equilibrium

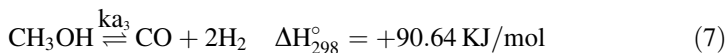
At higher pressures, methanol selectivities from carbon dioxide increased with increasing pressure over $\text{CuO}/\text{ZnO}/\text{Al}_2\text{O}_3$ catalyst. This tendency can be explained by the thermodynamic equilibrium for the related reaction. In particular, methanol synthesis over Cu-based catalysts proceeds exclusively via CO_2 hydrogenation and can be described by a reaction network involving the synthesis of methanol (5):



Simultaneously with methanol synthesis, the reverse water–gas shift reaction (RWGS) takes place depending on the reaction conditions (6):



The possible secondary reaction is (7):



Methane is the most thermodynamically favored product, and is generally undesirable economically (8):



The equilibrium constants, k_{a_1} , and k_{a_2} for reactions 1 and 2, were calculated from well-known thermodynamic relations and expressed in the following forms literature [28, 29]:

$$k_{a_1} = k_{a_2} \exp \left[22.225 + \frac{9143.6}{T} - 7.492 \ln T + 4.076 \times 10^{-3}T - 7.161 \times 10^{-8}T^2 \right]$$

where k_{a_1} is in atm^{-2} , and

$$k_{a_2} = \exp \left[13.148 + \frac{5693}{T} - 1.07 \ln T + 5.44 \times 10^{-4}T - 1.125 \times 10^{-7}T^2 + \frac{49170}{T^2} \right]$$

The k_a is a function of temperature only, while K_φ is a function of both temperature and pressure. This P, T dependence of K_φ is taken from Klier [8] in the following form,

$$K_{\varphi 1} = (1 - A_1 P)(1 - A_2 P)$$

$$K_{\varphi 2} = 1/(1 - A_2 P)$$

$$K_{\varphi 3} = K_{\varphi 2}/K_{\varphi 1} = 1/(1 - A_1 P)$$

where $A_1 = 1.95 \times 10^{-4} \exp\left(\frac{1703}{T}\right)$ and $A_2 = 4.24 \times 10^{-4} \exp\left(\frac{1107}{T}\right)$

The corresponding equilibrium equations are:

$$K_{P1} = \frac{(P_{CH_3OH})(P_{H_2O})}{(P_{CO_2})(P_{H_2})^3} \quad (9)$$

$$K_{P2} = \frac{(P_{CO})(P_{H_2O})}{(P_{CO_2})(P_{H_2})^3} \quad (10)$$

$$K_{P3} = \frac{(P_{CO})(P_{H_2})^2}{(P_{CH_3OH})} \quad (11)$$

Here, Eq. 7 represents a linear combination of Eqs. 5 and 6, and thus the thermodynamic evaluation depends on the analysis of Eqs. 5 and 6, although Eq. 7 can shed light on the CO/CH₃OH distribution [$k_{P3} = k_{P2}/k_{P1}$], where

$$k_{P1} = ka_1/k_{\varphi 1}; \quad k_{\varphi 1} = \varphi_{CH_3OH}\varphi_{H_2O}/\varphi_{CO_2}\varphi_{H_2}^3$$

$$k_{P2} = ka_2/k_{\varphi 1}; \quad k_{\varphi 2} = \varphi_{CO}\varphi_{H_2O}/\varphi_{CO_2}\varphi_{H_2}$$

$$k_{P3} = k_{P2}/k_{P1}; \quad k_{\varphi 3} = k_{\varphi 2}/k_{\varphi 1} = \varphi_{CO}\varphi_{H_2}/\varphi_{CH_3OH}$$

Fig. 6 shows the experimental and equilibrium constants in carbon dioxide hydrogenation as a function of reaction pressure over CuO/ZnO/Al₂O₃ catalyst. This figure clearly shows that equilibrium constants of methanol production from carbon dioxide (5) increased with increasing pressure (Fig. 6a), where CO production by reverse water–gas shift reaction (6) decreased with increasing pressure owing to the equilibrium (Fig. 6b). Under such conditions, CO₂ becomes a reactant of reaction 1 and a product in reaction 2. Hence the CO equilibrium constant becomes a negative

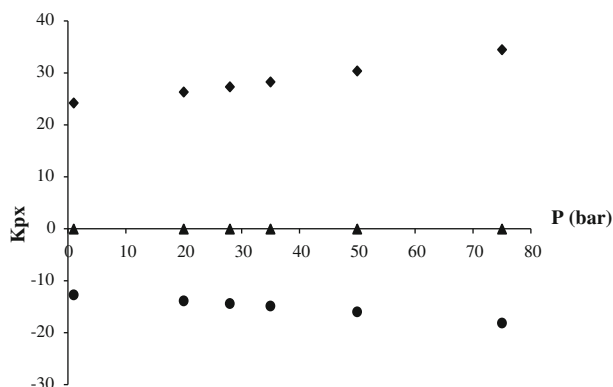


Fig. 6 Experimental and equilibrium constants in CO₂ hydrogenation as a function of pressure. **a** CO₂ + 3H₂ ⇌ CH₃OH + H₂O, **b** CO₂ + H₂ ⇌ CO + H₂O, **c** CH₃OH ⇌ CO + 2H₂

value, which means that some CO is converted into CO₂. Under such a condition, methanol decomposition to carbon monoxide (7) should also be in equilibrium (Fig. 6c). High temperature favors the endothermic reactions 6 and 7, whereas a high pressure favors reaction 5. Moreover, the methanol equilibrium constant is always higher, while the equilibrium constant of CO shows the opposite trend.

At a pressure of 75 bar, methanol selectivity reached 47%. This tendency can be explained by Le Chatelier's principle as the methanol synthesis reaction 5 proceeds under a volume contraction. Higher methanol selectivities are therefore obtained at higher pressures (Fig. 1).

The reaction between CO₂ and H₂ is exothermic. Reaction 5 is of interest for the methanol production from CO₂. Reaction 6 is competitive with this for the CO₂ conversion and it produces undesired CO, reducing the overall effectiveness of the process. Therefore, it is important to study the conversion of CO₂ and the methanol/CO selectivity. The selectivity of methanol/CO increases as the pressure increases, which shows that the impact of competitive reaction 6 is very insignificant.

Methanol selectivity increases with the pressure and decreases with the temperature. Thus, CO₂ produces mainly CO at low pressures and high temperature. It should be noticed that carbon dioxide can be hydrogenated at lower temperatures than carbon monoxide, which suggests that methanol can be formed directly from carbon dioxide at least in the lower temperature range. Methanol formation from carbon dioxide is always accompanied by carbon monoxide production. However, recent mechanistic studies of carbon dioxide hydrogenation over copper catalysts indicate that carbon dioxide is the main carbon source of methanol even from a carbon dioxide and carbon monoxide mixture [30, 31]. The experimental data were in fairly good agreement with the proposed mechanism.

Mechanism and pathway of CO₂ hydrogenation

The formation of methanol can be described by an adsorption–desorption mechanism. Previous studies on CuO/ZnO/Al₂O₃ [32–34] suggest that the formate and carbonate unideterminate or bideterminate species [35, 36] were formed when the Cu-based catalyst was exposed to CO₂/H₂ or CO/CO₂/H₂ at low temperatures, and carbonate species were transformed to stable formate species by hydrogenation which are then reduced to methoxy [37] and further hydrogenated to methanol. On the other hand, Fujitani et al. [38], who worked on the Pd/Ga₂O₃ catalyst, reported that surface formate and methoxy species were observed during CO and CO₂ hydrogenation. In contrast, the reaction pathway was clearly different between CO and CO₂ hydrogenation over the Pd/ZrO₂ catalyst. That is, surface formaldehyde and methoxy species were observed as intermediates during CO hydrogenation, while surface formate and methoxy species were detected during CO₂ hydrogenation.

The intermediates of CO₂ hydrogenation were carbonate (CO₃) formate (HCOO), carboxylate (HCOOH), methylenebisoxo (H₂COO) and methoxy (H₃C–O) species. This species was commonly detected in experiments [35–38].

Based on the observations noted above and in our experimental results, two mechanisms have been suggested to explain the formation of methanol and carbon

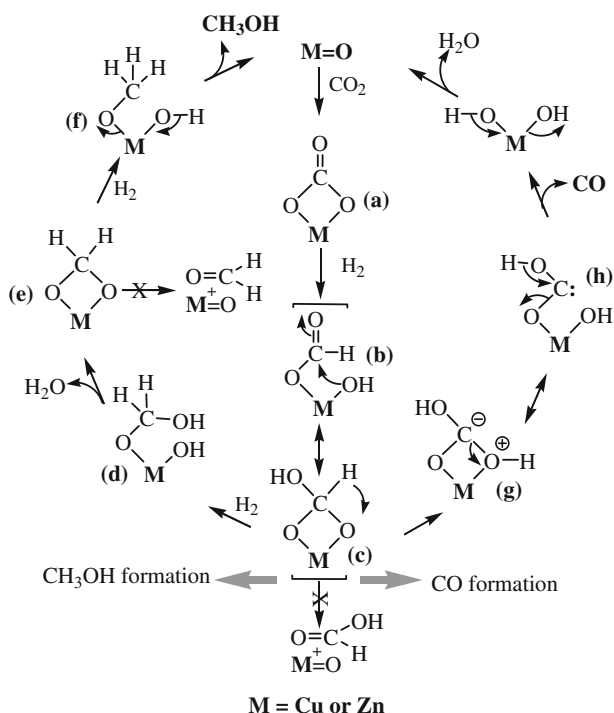


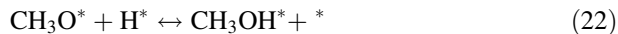
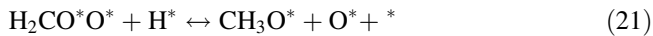
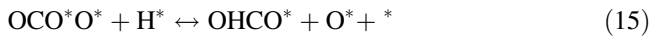
Fig. 7 Possible reaction pathways for CO_2 hydrogenation on $\text{M}=\text{O}$ oxide

monoxide over $\text{CuO}/\text{ZnO}/\text{Al}_2\text{O}_3$ catalyst. In the first mechanism (Fig. 7), adsorbed CO_2 reacts on the surface $\text{M}=\text{O}$ oxide with dissociatively adsorbed hydrogen in a series of hydrogenation steps to give methanol. Thus, the results suggest that adsorbed species were formed on single metal, M site.

In this scheme, methanol synthesis proceeds by prior formation of the carbonate (bidentate chelating) (a) adsorption species on the metal oxide, followed by hydrogenation of carbonate to the formate unideterminate (b). The formate monodentate (b) species is stable only at low temperatures ($<200^\circ\text{C}$) and is converted to the stable adsorbed bidentate chelating formic acid (c) through the reaction of $\text{C}=\text{O}$ group of formate (c) with OH groups adjacent [39]. The $\text{H}(\text{HO})\text{COO}$ (c) species is transformed easily to other intermediate such as $\text{H}_2(\text{OH})\text{C}-\text{O}$ (d) in the presence of hydrogen. The dehydration of $\text{H}_2(\text{OH})\text{C}-\text{O}$ (d) intermediate would give H_2COO (e), which reacts with H_2 to produce methoxy $\text{H}_3\text{C}-\text{O}$ (f) and methanol [40].

The intermediates $\text{H}(\text{HO})\text{COO}$ (c) and H_2COO (e) are formic acid and formaldehyde in the adsorbed state respectively over $\text{M}=\text{O}$ oxide. Formic acid and formaldehyde are not observed under our reaction conditions, we suggest that these compounds are adsorbed strongly on the surface of catalyst and transformed easily to other intermediates such as methylenebisoxo H_2COO (e) and methoxy $\text{H}_3\text{C}-\text{O}$ (f) respectively in the presence of hydrogen.

CH_3OH formation requires several steps through the formate pathway leading to the various adsorbed species [41] as follows:



In the second mechanism (Fig. 8), the first step is the insertion of CO_2 into a surface OH group with formation of surface bicarbonate (A). The HOCOO (A) intermediate can react with the surface hydroxyl group leading to the bidentate

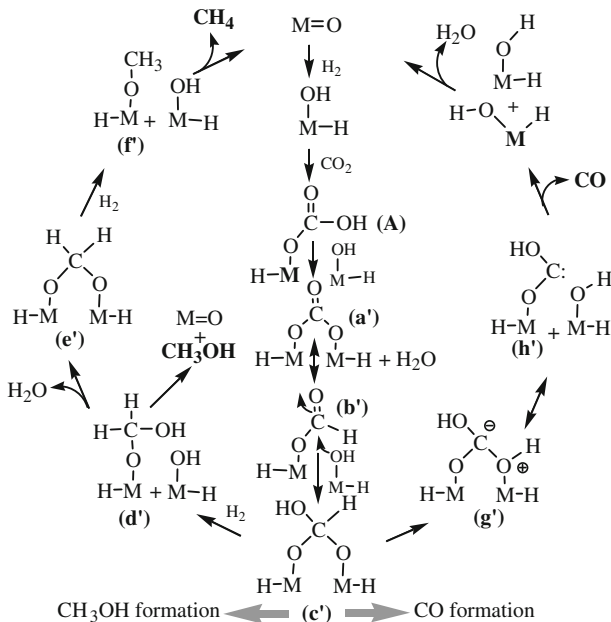


Fig. 8 Possible reaction pathways for CO_2 hydrogenation on $\text{MH}-\text{OH}$

carbonate (a') and H₂O. This is followed by further hydrogenation steps to give a surface H₂(HO)CO (d') species, from which methanol is formed. That adsorbed bidentate species was formed on the catalyst surface (Fig. 8) between two M sites.

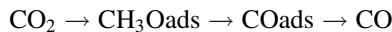
Both CH₃OH and CO are produced dominantly via the formate pathway as shown in Figs. 7 and 8. From the formate pathway, the formation of CO probably passes through the intermediate hydroxycarbene HO—C—Oads (h) which can dissociate into CO and H₂O via dehydration [42].

This clearly shows that the H(OH)COO (c) intermediate transfers hydrogen from carbon to a neighboring adsorbed oxygen atom, which inserts in the M—O—C bond leading to the formation of a stable carbanion (g) and transformed into adsorbed hydroxyl group and hydroxycarbene HO—C—O (h) [43] which is responsible for CO formation as shown in following pathway:



It appears that the adsorbed formic acid H(HO)COO (c) is the key intermediate in this reaction. It is responsible for both methanol and carbon monoxide formation. At low pressure, it is transformed predominantly into CO, while at high pressure it is transformed mainly into CH₃OH.

On the other hand, at low pressure CO seems to stem from the decomposition of methanol re-adsorbed as a methoxy species on a different site:



Whereas at high pressure, it appears to be produced directly from CO₂, in good agreement with thermodynamics which does not favor the decomposition of methanol into carbon monoxide.

Conclusion

The effect of pressure on CO₂ hydrogenation into methanol over CuO/ZnO/Al₂O₃ catalyst has been investigated.

Our results show a great influence of the operating pressure on the kinetics of the CO₂/H₂ reaction on CuO/ZnO/Al₂O₃ catalysts. The selectivity of methanol increases with the increase of pressure, suggesting that methanol is the primary product and is formed directly from CO₂.

CO₂ hydrogenation to methanol over M=O centers shows a consecutive pathway at low pressure (<35 bar) and parallel pathway at high pressure (>35 bar).

Both CH₃OH and CO are produced dominantly via the formate pathway, and the CO formation proceeds through a hydroxycarbene intermediate.

The thermodynamic analysis shows that the reaction of methanol formation from CO₂ is favored at high pressure rather than the reverse water–gas shift reaction (RWGS).

Open Access This article is distributed under the terms of the Creative Commons Attribution Noncommercial License which permits any noncommercial use, distribution, and reproduction in any medium, provided the original author(s) and source are credited.

References

1. Liu X-M, Lu G-Q, Yan Z-F, Beltramini J (2003) Ind Eng Chem Res 42:6518
2. Fujita S, Moribe S, Kanamori Y, Kakudate M, Takezawa N (2001) Appl Catal A Gen 207:121
3. Lim H-W, Park M-J, Kang S-H, Chae H-J, Bae J-W, Jun K-W (2009) Ind Eng Chem Res 48:10448
4. Liu X-M, Lu G-Q, Yan Z-F, Beltramini J (2003) Ind En Chem Res 42:6518
5. Song C (2006) Catal Today 115:2
6. Waugh KC (1992) Catal Today 15:51
7. Bart JCJ, Sneeden RPA (1987) Catal Today 2:1
8. Klier K (1982) Adv Catal 31:243
9. Klier K, Chatikavanij V, Hermann RG, Simmons GW (1979) J Catal 56:407
10. Schack CJ, McNeil MA, Pinker G (1989) Appl Catal 50:247
11. Chinchen GC, Waugh KC, Whan DA (1986) Appl Catal 25:101
12. Chinchen GC, Mansfield K, Spencer MS (1990) Chemtech 20:692
13. Lee S, Parameswaran V, Wender R, Kulik I (1989) Fuel Sci Technol Int 7:1021
14. Liu G, Wilkox D, Garland M, Kung HH (1984) J Catal 90:139
15. Fujita S, Usui M, Ohara E, Takezawa N (1992) Catal Lett 90:349
16. Ramaroson E, Kieffer R, Kienemann A (1982) Appl Catal 4:281
17. Tagawa T, Pleizer G, Amenomiya Y (1985) Appl Catal 18:285
18. Ipatieff VN, Monroe GS (1945) J Amer Chem Soc 67:2128
19. Denise B, Cherifi O, Bettahar MM, Sneeden RPA (1989) Appl Catal 48:365
20. Rozovski YaA, Kagan YuB, Lin GI, Loctev SM, Slivinski EV, Liberov LG, Bashkirov AN (1975) Kinet Katal 16:810
21. Bardet R, Thivolle-Cazat J, Trambouze Y (1981) J Chim Phys 78:1351
22. Baussart H, Delobel R, Lebras M, Le Maguer D, Leroy JM (1985) Appl Catal 14:381
23. Evans JW, Wainwright MS, Bridgwater AJ, Young DJ (1983) Appl Catal 7:75
24. Rasmussen PB, Holmlad PM, Askgaard T, Ovesen CV, Stoltze, Nørskov JK, Chorkendorff I (1994) Catal Lett 26:373
25. Rasmussen PB, Kazuta M, Chorkendorff I (1994) Surf Sci 318:267
26. Fisher IA, Bell AT (1997) J Catal 172:222
27. Weigel J, Koeppl RA, Baiker A, Wokaun A (1996) Langmuir 12:5319
28. Chinchen GC, Denny PJ, Jennings JR, Spencer MS, Waugh KC (1988) Appl Catal 36:1
29. Bisset L (1977) Chem Eng 84:155
30. Chichen GC, Denny PJ, Parker DG, Spencer MS, Whan DA (1987) Appl Catal 30:33
31. Muhler M, Törnqvist E, Nielsen LP, Clausen BS, Topsøe H (1994) Catal Lett 25:1
32. Bailey S, Froment GF, Snoek JW, Waugh KC (1995) Catal Lett 30:99
33. Nakamura J et al (1995) Catal Lett 31:325
34. Fujita S, Usui M, Ito H, Takezawa N (1995) J Catal 157:403
35. Browner M, Hadden RA, Houghton H, Hyland JNK, Waugh KC (1988) J Catal 109:263
36. Millar GJ, Rochester CH, Waugh KC (1992) Catal Lett 14:289
37. Kienemann A, Idriss H, Hindermann JP, Lavalle JC, Vallet A, Chaumette P, Courty Ph (1990) Appl Catal A 59:165
38. Fujitani T, Nakamura I (2002) Bull Chem Soc Jpn 75:1393
39. Chen X, Goodman DW (1996) J Phys Chem 100:1753
40. Gao LZ, Au CT (2000) J Catal 189:1
41. Vanden Bussche KM, Froment GF (1996) J Catal 161:1
42. Hu S-W, Wang X-Y, Chu T-W, Liu X-Q (2005) J Phys Chem A 109:9129
43. Hu SW, Lu SM, Wang XY (2004) J Phys Chem A 108:8485